J Physiol (2003), **550.1**, *pp.* 123–133
DOI: 10.1113/jphysiol.2002.038737

www.jphysiol.org

Journal of Physiology

Development of synchronized activity of cranial motor neurons in the segmented embryonic mouse hindbrain

J. Gust, J. J. Wright, E. B. Pratt and M. M. Bosma

Department of Zoology, Box 351800, University of Washington, Seattle, WA 98195-1800, USA

Spontaneous electrical activity synchronized among groups of related neurons is a widespread and important feature of central nervous system development. Among the many places from which spontaneous rhythmic activity has been recorded early in development are the cranial motor nerve roots that exit the hindbrain, the motor neuron pool that, at birth, will control the rhythmic motor patterns of swallow, feeding and the oral components of respiratory behaviour. Understanding the mechanism and significance of this hindbrain activity, however, has been hampered by the difficulty of identifying and recording from individual hindbrain motor neurons in living tissue. We have used retrograde labelling to identify living cranial branchiomeric motor neurons in the hindbrain, and $[Ca^{2+}]_i$ imaging of such labelled cells to measure spontaneous activity simultaneously in groups of motor neuron somata. We find that branchiomeric motor neurons of the trigeminal and facial nerves generate spontaneous $[Ca^{2+}]_i$ transients throughout the developmental period E9.5 to E11.5. During this two-day period the activity changes from low-frequency, long-duration events that are tetrodotoxin insensitive and poorly coordinated among cells, to high-frequency short-duration events that are tetrodotoxin sensitive and tightly coordinated thoughout the motor neuron population. This early synchronization may be crucial for correct neuron–target development.

(Received 31 December 2002; accepted after revision 4 April 2003; first published online 2 May 2003)
Corresponding author M. M. Bosma: Department of Biology, Box 351800, University of Washington, Seattle, WA 98195-1800, USA. Email: martibee@u.washington.edu

In the highly cephalized animal, some muscles of the face derive from mesoderm originating in the branchial arches, hence the name branchiomeric muscle. In addition to the normal complement of motor neurons, the hindbrain has a unique population of branchiomeric motor neurons to control these muscles. These motor neurons are specified by defined homeobox transcription factors (Varela-Echavarria *et al.* 1996) and are found only in the hindbrain. During early development, the hindbrain is transiently segmented into rhombomeres (Lumsden & Keynes, 1989; Lumsden, 1990; Guthrie, 1996; Trainor & Krumlauf, 2001), developmental compartments that restrict neuronal migration (Fraser *et al.* 1990). In mice, rhombomeric segregation is present from approximately embryonic day 8 (E8) to E11.5. Two cranial nerves that include branchiomeric components are the trigeminal (V), originating in rhombomeres r2 and r3, and the facial (VII), originating in r4 and r5 at E9–10 (Pierce, 1973; Guthrie & Lumsden, 1992). The outputs of these cranial nerves coordinate important rhythmic motor activities, such as suckling in mammals, swallowing, mastication, speech and the oral components of respiration.

Recordings from cranial nerve roots in chick and mouse indicate that branchiomeric motor neurons generate spontaneous, rhythmic activity in the post-segmented hindbrain, which develops synchronicity across previous rhombomeric boundaries (Fortin *et al.* 1995; Jacquin *et al.* 1999; Abadie *et al.* 2000). It is likely that this coordinated activity plays an important role in the development of hindbrain circuitry and physiology, as it does in other CNS structures (Ben-Ari, 2001). Early rhythmic activity in these cells is also particularly interesting because this output in the newborn animal controls required rhythmic behaviour, such as suckling and swallowing. However, the mechanisms that generate and synchronize this hindbrain activity have been hard to study because it is difficult to identify individual branchiomeric motor neurons in living tissue and to record activity simultaneously from many individual motor neuron somata, the probable sites where activity is controlled.

We have used $[Ca^{2+}]_i$ imaging methods to monitor activity simultaneously in multiple, branchiomeric motor neurons identified by retrograde labelling in the embryonic mouse. Our goal was to record spontaneous activity in these motor

neurons at very early stages of development, before axonogenesis is complete, to determine whether the developmental onset of spontaneous activity could be monitored. We show that very early in development (E9.5), during the period of rhombomeric segmentation, these neurons begin to generate spontaneous $[Ca^{2+}]_i$ transients. These transients rapidly change character over the next 48 h, becoming shorter in duration and more frequent. At the end of this period, these transients become synchronized among motor neurons rather abruptly between E11.0 and E11.5, just at the end of rhombomeric segmentation. We further show that as this activity becomes synchronous it also becomes sensitive to TTX block, implying that the basic ion channel mechanisms that underlie this activity change as synchronization develops

METHODS

Animals and solutions

Timed-pregnant mice (embryonic day 0.5 (E0.5) defined as the morning after plug formation) were killed by an excess of CO_2 in accordance with the regulations of the University of Washington Animal Care Committee (IACUC), and embryos dissected and staged by Theiler stages according to characteristics listed in the Edinburgh Mouse Atlas

(http://genex.hgu.mrc.ac.uk/Databases/Anatomy).

We used staging by Theiler criteria because it is more precise than staging by plug time; we then named the embryos by nominal embryonic day (E). Thus, Theiler stage 15 corresponds to E9.5, Theiler stage 16 to E10.0, etc. The same person staged all the animals to remove any investigator variability. As individual embryos within one litter differ in developmental stages, each embryo was staged independently. A few of the experiments used the C57/Bl6 strain of mouse, but the majority of experiments were performed on Swiss/Webster mice. No differences in the physiological results were observed between strains.

The dissecting and recording solution was artificial cerebral spinal fluid (ACSF) containing (mM): 119 NaCl, 8 KCl, 1.3 $MgCl_2$, 2.5 $CaCl_2$, 1.0 NaH_2PO_4, 26.2 $NaHCO_3$, 11 glucose, and was bubbled continuously with a mixture of 95 % O_2– 5 % CO_2 (carbogen). The pH of the bubbled equilibrated solution was pH 7.3. The targets of the trigeminal and facial motor nerves (branchial arches 1 and 2, respectively) were injected with Texas-Red (TR)-conjugated, lysine-fixable dextran (molecular mass 3000 Da, Molecular Probes, Eugene, OR, USA) using a 37 gauge needle. The animals were then rinsed repeatedly to remove residual dextran, and incubated in bubbled ACSF for 1.5–8 h at room temperature to allow retrograde transport of the dextran. Dextran label uptake into nerve endings is via activity-dependent endocytosis, which is increased when neuron activity is increased by relatively high levels of K^+ in the exernal solution (Jiang *et al.* 1993; Reiner *et al.* 2000). Transport along the axon may include an element of diffusion, and thus, the signal near the nucleus may appear compartmentalized. For whole hindbrain experiments (younger animals), the facial mesenchyme was removed, the hindbrain opened along the dorsal midline and laid dorsal side down in the recording chamber (open hindbrain preparation). For older animals, where the ventricular zone of the tissue is thicker and impedes the visualization of labelled neurons, the entire animal was embedded in low temperature gelling agar at 35° C, (Sigma, St Louis, MO, USA), chilled and sliced in a vibratome into 200 μm slices.

$[Ca^{2+}]_i$ imaging

Whole hindbrains or slices were incubated in bubbling ACSF at room temperature containing 1.75 μM of the $[Ca^{2+}]_i$ indicating dye fluo-4 and 0.07 % pluronic-127 (Molecular Probes, Eugene, OR, USA) for 15 min. Tissue was then rinsed and placed into a glass-bottomed chamber on the stage of an inverted microscope, with continuous perfusion by carbogen-bubbled ACSF. The dextran-loaded cells were imaged with 594 nm excitation, and the fluo-4 signal monitored with 488 nm excitation. Individual cells were chosen and the average $[Ca^{2+}]_i$ signal for each cell recorded every 10 s using the software package MetaFluor (Universal Imaging, West Chester, PA, USA). This sampling regime was the optimal compromise between signal bleaching and temporal resolution of the signal over long time periods.

Data analysis

$[Ca^{2+}]_i$ signals were analysed in Sigmaplot (SPSS Science, Chicago, IL, USA) for general trend observations, and subtracted by an off-tissue sample to remove system drift from traces. Data were then transferred to Matlab (Mathworks, Natick, MA, USA), where analysis for transient durations, intervals, and synchronization of events was performed. Data were filtered with a 4-pole Bessel filter to remove low-frequency baseline drift and dye bleaching and then put through a threshold analysis program, to measure the durations of $[Ca^{2+}]_i$ transients and the intervals between peaks. For each cell, threshold was set at 10 % of the maximal $[Ca^{2+}]_i$ transient (dotted line in top panels in Fig. 2*A* and *B*). The records were then idealized into binary form, with 1 for times that the record was above threshold and 0 for times that the record was below threshold (idealized records in middle panels in Fig. 2*A* and *B*). Durations were measured as the time the event was above threshold, while intervals were measured as the time between the end of one event and the crossing of threshold starting a new event. Synchronization between neurons was quantified by summing the idealized records of all active cells in each recording (4–12 cells), and dividing by the number of cells to get the average activity; thus, if a given event occurred simultaneously in all cells, the idealized summed transient would have an amplitude of 1.0 (or 100 % of the cells). A synchronization value (SV) was then assigned by dividing the number of averaged events above 0.7 (events in which 70 % of the cells had simultaneous transients) by those above 0.2 (events in which only 20 % of the cells participated with simultaneous transients). See bottom panels in Fig. 2*A* and *B*.

Immunocytochemistry

Animals used for physiology and their injected littermates were analysed by immunocytochemistry (ICC). The tissue was fixed in chilled freshly-made 4 % paraformaldehyde in phosphate buffered saline (PBS, in mM: 3.16 NaH_2PO_4, 6.84 Na_2HPO_4, 0.15 NaCl, pH 7.2) for 1 h. Whole hindbrains were evaluated as tissue blocks or slices. Tissue was blocked for 1 h with 5 % normal goat serum (Jackson ImmunoResearch Laboratories, West Grove, PA, USA), and incubated overnight with primary antibodies to examine the expression of the motor neuron-specific transcription factor Islet-1 (Ericson *et al.* 1992) (monoclonal 39–4D5, 1:100, obtained from Developmental Studies Hybridoma Bank, Iowa City, IA, USA), or for neuron-specific class III beta-tubulin (TuJ1, 1:500; Moody *et al.* 1987) (polyclonal

antibody, Covance, Princeton, NJ, USA) to confirm the dextran-labelled cells as motor neurons or neurons, respectively. The secondary label was goat-anti-rabbit or -mouse Alexa 488 (Molecular Probes, Eugene, OR, USA), used at 1:200 for one hour. Tissue was examined in a confocal microscope (BioRad, Hercules, CA, USA) and images manipulated with Adobe Photoshop (Adobe Systems, San Jose, CA, USA).

RESULTS

Identification of motor neurons in living tissue for $[Ca^{2+}]_i$ imaging

The motor neurons of the trigeminal and facial nerves are somewhat larger than other cells within the hindbrain and their locations can be roughly approximated by the rhombomere location. Nevertheless, more certain identification is useful since these neurons also migrate within the hindbrain over this developmental period and there are other cell types present. We identified motor neurons by injecting their target tissue with a Texas Red-labelled dextran.

At stages E9.5–10.0, there were few dextran-labelled cells in the hindbrain, even with prolonged incubation. Confocal examination of cross sections treated for TuJ immunoreactivity at these early stages showed that few hindbrain motor axons had extended fully to the periphery, and thus the dextran in the target regions often was not able to reach the hindbrain. At these early stages, the motor neurons were identified by dextran label, if present, or by their large size and position within specific rhombomeres, as determined by immunocytochemical identification of those sites using Islet-1 immunostaining. At E9.5, Islet-1-positive neurons are seen medially in much of the hindbrain, and more laterally in the central regions of rhombomere r2 (data not shown). In older animals, dextran injection into target regions labelled more neurons (as seen in Fig. 1*E* and *F*), and we used both the dextran-labelled neurons and nearby cells for $[Ca^{2+}]_i$ experiments. Dextran-identified neurons were included in the general pool of cells, as well as shown separately on each graph (open columns, Figs 3 and 5).

Spontaneous $[Ca^{2+}]_i$ transients in branchiomeric neurons

At all stages examined (E9.5-E11.5), branchiomeric motor neurons generated repeated spontaneous $[Ca^{2+}]_i$ transients. Figure 1*A* shows three cells recorded from an E9.5 hindbrain, in rhombomere 4, near one dextran-labelled neuron from a b2 injection (the dextran-labelled cell itself was not active). $[Ca^{2+}]_i$ transients in each cell are long in duration, with long intervals between transients. At E10.5 (Fig. 1*B*), the two dextran-identified neurons (shown in Fig. 1*E*) generated shorter-duration transients, although they were still infrequent. At E11.0 (Fig. 1*C*; some of the dextran-labelled cells shown in Fig. 1*F*) and E11.5 (Fig. 1*D*) each of the four neurons shown generated short duration transients, and did so more frequently. To ascertain that the dextran-labelled cells were indeed branchiomeric neurons, immunocytochemistry for Islet-1, a motor neuron-specific transcription factor, was done on fixed tissue samples. Figure 1*G* shows an E11.5 hindbrain slice that was labelled by b1 injection of dextran. The incoming dextran-labelled axons (red) lead into the lateral branchiomeric motor pool, and are double-labelled with Islet-1 (green) indicating that they are motor neurons that have migrated from near the midline to the lateral portion of the hindbrain. A few labelled neurons' somata (arrows) have not yet translocated to the lateral pool.

To quantify the basic properties of the $[Ca^{2+}]_i$ activity over developmental time, we used a threshold detection routine to create idealized representations of the transients in each cell record (see Methods). Figure 2*A* and *B* illustrates this method for representative cells at E9.5 (upper three panels) and E11.5 (lower three panels). The top panels of each stage ($\Delta F/F$) show the baseline-subtracted $[Ca^{2+}]_i$ records for individual cells, with detection thresholds indicated by the dashed lines. The middle panels show the idealized records from these individual cells generated by the detection program, and from these we measured the duration of each transient, the intervals between transients, and the correlation of transients among motor neurons in the population sampled. (See below for descriptions of the bottom panels of Fig. 2*A* and *B*.)

The pattern of activity of the earliest embryonic motor neurons consists of relatively infrequent, long-duration single transients, or short trains of transients. The transient $[Ca^{2+}]_i$ elevations in all neurons at E9.5 had a mean duration of 80.4 ± 4.2 s (n = 288 events; Fig. 3*A*). Between E9.5 and E11.5, the duration of individual transients decreased (compare Fig. 1*A* to 1*B, C* and *D*), reaching a mean duration of 12.6 ± 0.24 s at E11.5 (n = 1271 events; Fig. 3*A*, filled columns). Over the same developmental time, the interval between individual $[Ca^{2+}]_i$ transients also decreased (compare traces in Fig. 1*A, B, C* and *D*), from 294 ± 21 s (n = 256 events) at E9.5 to 82.2 ± 2.4 s (n = 1229 events) at E11.5 (Fig. 3*B*, filled columns). Thus the developmental trend is towards more frequent, but shorter $[Ca^{2+}]_i$ transients in a given time period. Analysis of the subset of the population consisting only of retrogradely labelled neurons demonstrated the same trend, indicating that the nearby but unlabelled neurons are similar in behaviour to identified branchiomeric motor neurons, and are most likely also motor neurons. Given that the dextran injection into the target tissue does not cover the entire target area innervated by the motor pool at a given point in time, it is not surprising that a relatively small population of the motor pool is dextran identified. The total numbers of cells

at each stage on which this analysis was performed is shown in the figure legend.

Development of synchronization among neurons

One of the most dramatic developmental changes in the pattern of $[Ca^{2+}]_i$ transients between E9.5 and E11.5 is the appearance of synchronicity among the motor neurons in the population. Figure 4 shows longer records from the same neurons shown in portions *C* and *D* of Fig. 1, over a longer recording time and offset in order to better observe activity in individual cells. In an E11.0 hindbrain, the two lower cells are synchronous at many time points (although the relative

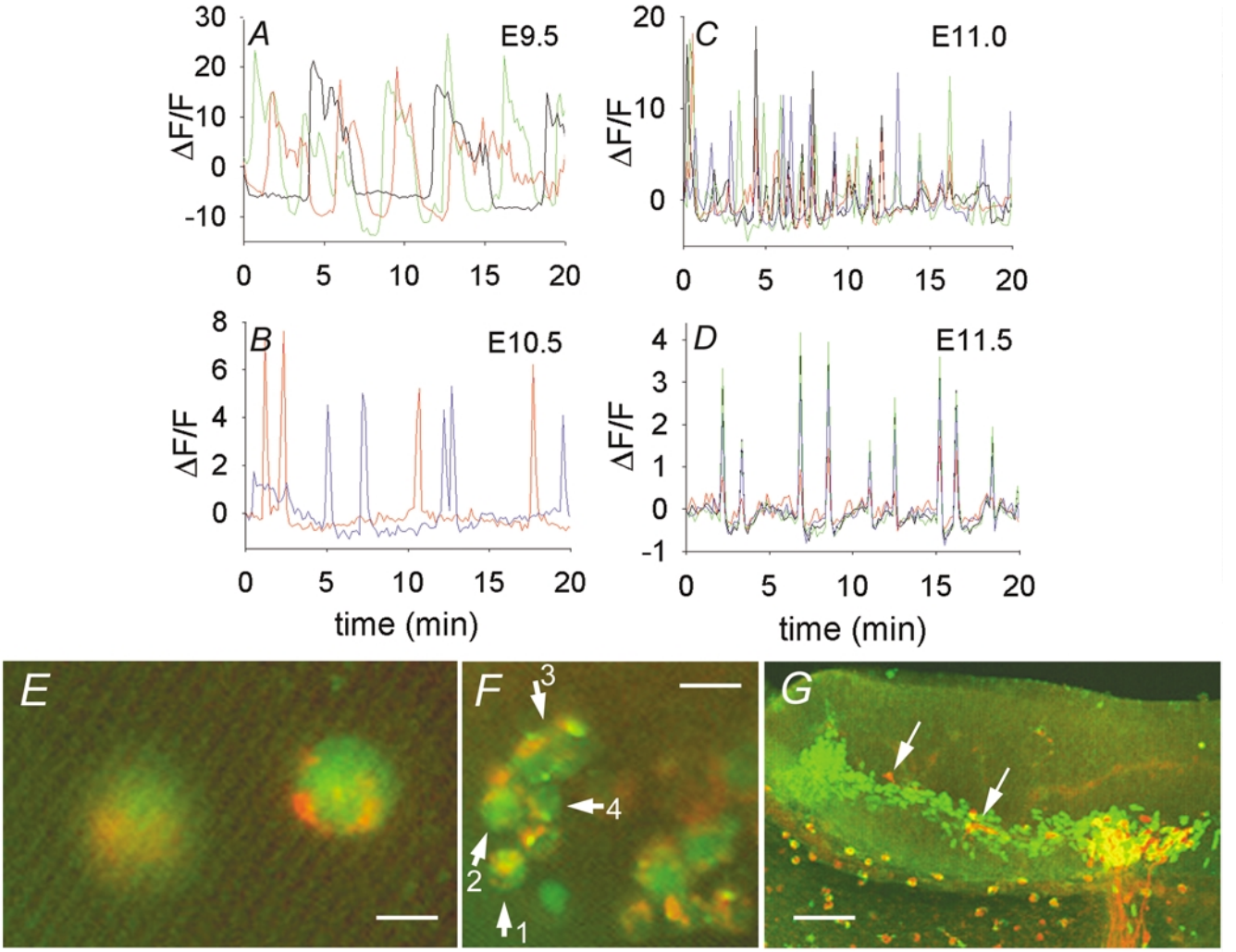

Figure 1. Embryos of different stages with dextran-labelled motor neurons loaded with fluo-4 and the $[Ca^{2+}]_i$ traces from those neurons

A, stage E9.5 embryo, branchial arch 2 injection, open hindbrain preparation. Recordings from cells within medial area of rhombomere 4 (r4), near a single dextran-identified neuron from a b2 injection. Each colour represents the activity from a different neuron. Note the slow oscillations in $[Ca^{2+}]_i$ and lack of coordinated activity between cells. *B*, stage E10.5 C57/Bl6 embryo, branchial arch 1 injection, open hindbrain preparation. Note the long intervals between $[Ca^{2+}]_i$ transients in these two neurons, which were near to each other. *C*, stage E11.0 C57/Bl6 embryo injected in branchial arch 1, open hindbrain preparation. Cells are active with many $[Ca^{2+}]_i$ transients and shorter intervals between transients. Some cells are active simultaneously with others. *D*, stage E11.5 embryo, 200 μm transverse slice, injected in branchial arch 2. $[Ca^{2+}]_i$ transients from individual cells are completely synchronized. *E*, cells from which activity in *B* was obtained, showing the dextran label (red) and fluo-4 signal (green) overlapping in the somata. Scale bar is 20 μm. *F*, group of dextran-labelled neurons, arrows indicate neurons from which records are shown. Numbers correspond to traces offset for clarity in Fig. 4. Scale bar is 40 μm. *G*, fixed E11.5 slice, showing dextran-labelled axons (red) extending from the lateral trigeminal motor pool after injection into b1. Green signal is staining for expression of Islet-1, and both the medial and lateral motor pools are stained. Axons exit only from the lateral motor pool; a few neuron somata that are migrating laterally (arrows) are dextran identified with axons exiting laterally. Scale bar is 75 μm.

amplitudes of the events vary), while the two upper cells show much less synchronicity either with each other or with the lower two cells. The lower panel shows that at E11.5, activity is highly synchronized among the four cells.

Synchronization of $[Ca^{2+}]_i$ transients between cells within each experiment was quantified by averaging the idealized records from all active cells within a single experiment (Fig. 2; see Methods). This is illustrated in Fig. 2*A* for an E9.5 stage animal, where there is little synchronization between cells, and for an E11.5 stage animal (Fig. 2*B*), where the synchronization is high. At E9.5, the population-averaged idealized record (bottom panel at E9.5) is dominated by low-amplitude events, indicating that only a small percentage of the cells participate in any given transient. At E11.5, in contrast, the population-averaged record (bottom panel at E11.5) is dominated by events >0.8 in amplitude, indicating that more than 80 % of the active cells in the sample participate in most events. The number of events in the averaged record that are greater than 0.7 (indicating that more than 70 % of the cells

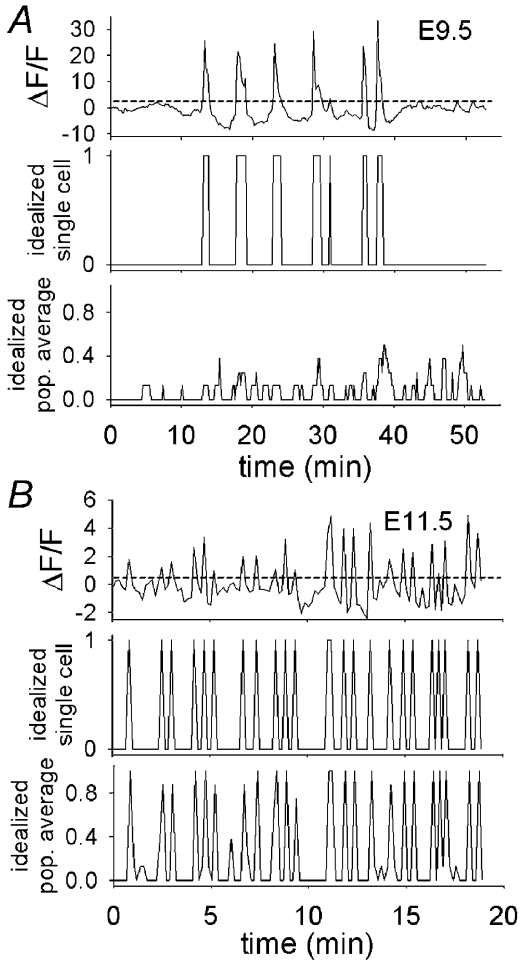

Figure 2. Method of analysis of event durations, intervals and degree of synchronization

A, three panels from E9.5 embryo. *B*, three panels from E11.5 embryo. Dashed line in top trace of *A* and *B* of baseline-subtracted records indicates threshold, and each middle panel shows the idealized record of the trace in the top panels. The durations of events were measured as the time above threshold, the intervals were times between transients. For measurement of synchronization between cells, idealized $[Ca^{2+}]_i$ transient records from eight individual cells were averaged as shown in bottom panels of *A* and *B* (population-averaged idealized record, bottom panels for both stages), and a synchronization value (SV) calculated. SV is 0.00 for the E9.5 embryo (*A*) and 0.89 for the E11.5 embryo (*B*).

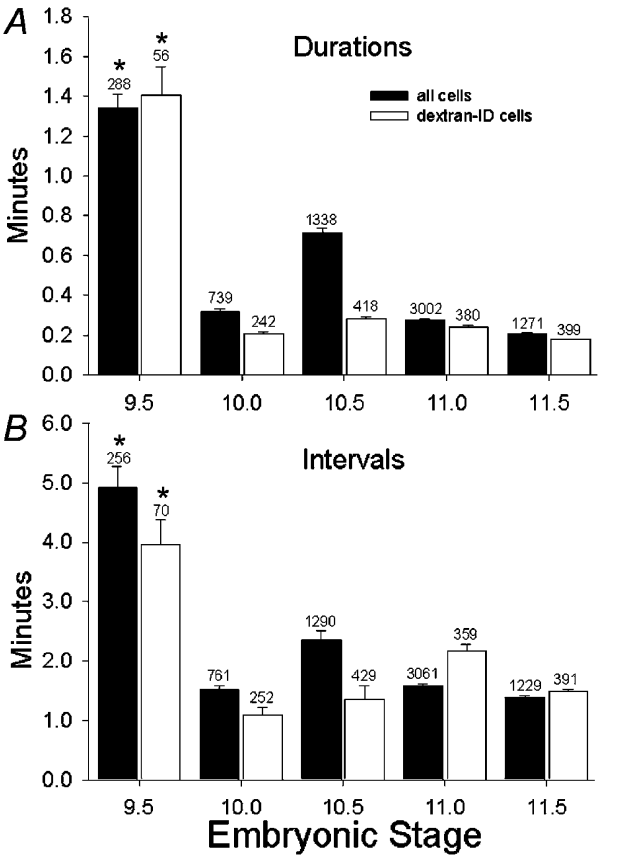

Figure 3. Quantification of $[Ca^{2+}]_i$ transient durations and intervals over developmental stages E9.5 to E11.5

A, durations of individual transients in all neurons from different developmental stages (filled columns), and the subset of dextran-identified neurons from the same experiments (open columns). The values at E9.5 (both all cells and dextran-identified cells) are significantly greater than all other stages ($P < 0.000004$). No other groups are significantly different. Error bars are S.E.M., numbers above columns are numbers of events. *B*, intervals between events shown for different developmental stages for events in all neurons (filled bars) and in dextran-identified neurons (open bars). The values at E9.5 (both all cells and dextran-identified cells) are significantly greater than all other stages ($P < 0.000004$). No other groups are significantly different. Error bars are S.E.M., numbers above columns are numbers of events. Numbers of cells are: E9.5: total, 43; dextran, 9; E10.0: total, 49; dextran, 17; E10.5: total, 114; dextran, 23; E11.0: total, 200; dextran, 36; E11.5: total, 47; dextran, 23.

participated in an event) was divided by the number of events that are greater than 0.2 (indicating that an event has occurred) and was assigned the synchronization value (SV) for that population. With this method, the SV is the percentage of events in which 70 % of the population of cells participate synchronously in a given $[Ca^{2+}]_i$ transient.

Results from embryos at different stages show that the SV showed no significant change from E9.5 to E11.0 and a highly significant increase between E11.0 and E11.5 (filled columns, Fig. 5). This trend was also observed in analysis of the subset composed exclusively of dextran-identified cells within particular experiments (open columns, Fig. 5). The total number of cells is shown in the figure legend for each stage and for the subset of dextran-identified cells. The number of cells is lower than that for which the kinetic analysis is performed, because of experiments which had between one and three cells, and on which synchronization analysis was not performed.

Synchronization between neurons is observed at a point where the ventricular zone tissue has thickened, so most experiments in older animals were performed in 200 μm hindbrain slices, whereas earlier experiments were performed in the open-hindbrain preparation. In order to rule out the possibility that synchronization was not a result of slicing the tissue, younger embryo hindbrains were sliced for experimentation. In these younger animals, such as the E10.5 animal shown in Fig. 6*A*, we did not observe any more synchronization than in the open-hindbrain preparation (data not shown; $n = 3$). The converse experiment was also performed, where the older intact hindbrain was carefully dissected free of facial mesenchyme in order to make the tissue as thin as possible. Under these conditions, synchronicity was observed in dextran-identified neurons (data not shown; $n = 6$). Thus, the technique of slicing the tissue does not induce the expression of synchronized activity between motor neurons.

These experiments were performed in an external solution with 8 mM K^+. This was used in order to increase the uptake of dextran into the neurons to facilitate more labelling and identification. In two sets of experiments at E11.5, we used external solutions with 2.5 mM K^+, and found that activity and synchronization were consistently present, and within the same range of frequencies, as in the experiments using 8 mM K^+ (data not shown).

Development changes in the ionic basis of activity

To test whether changes in transient duration, frequency and synchronicity are accompanied by underlying changes in the basic mechanisms of $[Ca^{2+}]_i$ transient generation, we

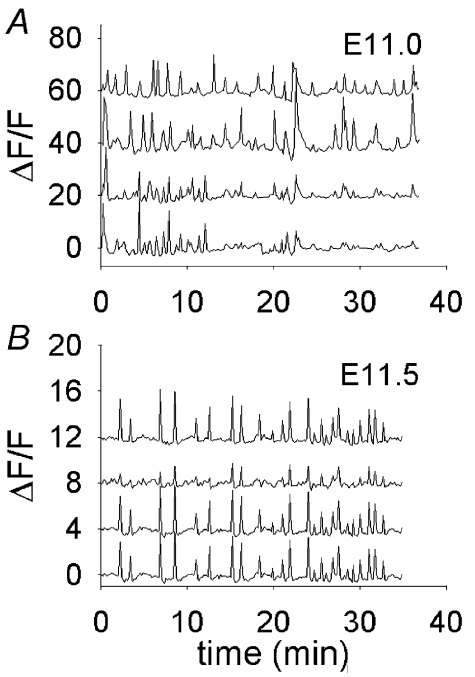

Figure 4. Offset records from experiments shown in Fig. 1*C* and *D* over longer time recordings to compare synchronicity of individual events

A, records of activity from neurons 1–4 (plotted bottom to top). Some synchronization is observed at E11.0. *B*, records of activity from E11.5 experiment in Fig. 1*D*; complete synchronization of all events is observed.

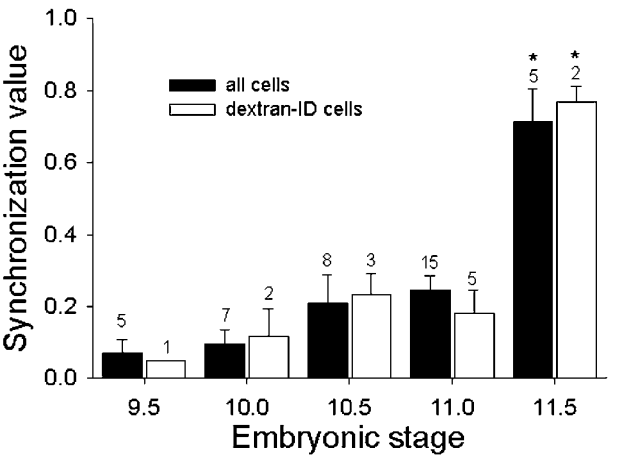

Figure 5. Synchronization values change over developmental time

Synchronization values for all active cells in experiments at different developmental stages are shown in filled columns, while synchronization between those cells that are dextran identified is shown in the open columns. Error bars are S.E.M.; numbers above columns are number of experiments (4–12 neurons per experiment). The E11.5 'all-cell' data are significantly different ($P < 0.0001$) when compared to all cells at other stages. The E11.5 dextran-identified cells are significantly different ($P < 0.001$) when compared to dextran-identified cells at other stages. Significance was determined using a Tukey HSD Least Squares Mean test, which compares the heterogeneity of all groups. Numbers of cells are: E9.5: total, 26; dextran, 7; E10.0: total, 36; dextran, 10; E10.5: total, 64; dextran, 17; E11.0: total, 152; dextran, 31; E11.5: total, 43; dextran, 20.

exposed cells at early and late stages to tetrodotoxin (TTX) to block voltage-gated Na^+ channels. Figure 6*A* shows an experiment in a sliced hindbrain from an E10.5 embryo, where asynchronous, infrequent $[Ca^{2+}]_i$ transients are not blocked by application of 300 nM TTX ($n = 2$ experiments). In contrast, one day later, the regular and synchronous $[Ca^{2+}]_i$ transients are completely and reversibly blocked by 150 nM TTX (Fig. 6*B*; $n = 3$ experiments). Application of TTX not only blocks synchronous transients, but most $[Ca^{2+}]_i$ transients in the tissue. Thus, in the same time period that synchronization appears, the molecular basis of excitation appears to change as well.

DISCUSSION

We have used $[Ca^{2+}]_i$ imaging methods to measure spontaneous activation of branchiomeric motor neurons of the trigeminal and facial nerves in the embryonic mouse hindbrain, identified by retrograde TR-dextran labelling. We have observed that between E9.5 and E11.5, these neurons generate spontaneous $[Ca^{2+}]_i$ transients, which change dramatically over this short developmental interval. At E9.5, they are long in duration, occur at relatively low frequency and are rarely synchronized among cells. From E9.5–E11.5, the mean duration of transients decreases by approximately fivefold, and the mean interval decreases by approximately threefold. In addition, between E11.0 and E11.5, the transients become abruptly synchronized within the motor neuron population, with an average of 75 % of cells participating in a given single event. Correlated with this abrupt appearance of synchronicity, the transients become sensitive to block by TTX.

Spontaneous and synchronous activity are driven by local circuits

The mechanism of generation of the spontaneous activity underlying these $[Ca^{2+}]_i$ transients in mouse hindbrain is probably endogenous to the hindbrain itself, since at all time points the stage-appropriate transients were recorded either in whole hindbrain preparations or in slices, both which preparations would eliminate influences from other brain regions. In chick hindbrain after the period of rhombomeric segmentation (Hamburger-Hamilton stages 24–36; Fortin *et al.* 1995), and mouse hindbrain (E10.5–E14.5; Abadie *et al.* 2000) rhythmic patterns occur in coactivated branchiomeric cranial nerve roots, which alter over developmental time. The rhythmic pattern is intrinsic to the local hindbrain regions, since the pattern remained (slightly altered in frequency) in isolated segments of the hindbrain in the chick (Fortin *et al.* 1994). Thus, neither spontaneous activity nor synchronization between nerve roots require the inputs from a higher-level central pattern generator, but originate within local circuits.

At these stages of development in mouse hindbrain, two descending tracts, the medial longitudinal fascicularis (mlf) and the lateral longitudinal fascicularis (llf), have extended into the entire hindbrain (Easter *et al.* 1993; Mastick & Easter, 1996; Glover, 2000), but the presence and types of synaptic connections between the longitudinal tracts and motor neurons have not been reported. It is probable that the $[Ca^{2+}]_i$ transients that we recorded in the mouse and the synchronization observed between neurons are not a function of higher-order networks but rather are the result of local circuits and electrical coupling. At E10.5–11.5, connexin 31 (Cx31) expression is found in r3, r5 and in the points of nerve entry and exit in several of the cranial nerves at E11.5. In addition, at E10.5–11.5, connexin 36 (Cx36) is expressed in neurons that appear to be the contralateral vestibuloacoustic efferent neurons in r4 and in ventral neurons in r5 in the position of facial motor neurons (Jungbluth *et al.* 2002). This shows that the proteins that subserve electrical coupling are probably present in facial branchiomeric neurons at the point when neurons are synchronously active.

Changes in ion channel expression probably mediate changes in $[Ca^{2+}]_i$ transients

The long-duration $[Ca^{2+}]_i$ transients recorded at E9.5 are TTX insensitive. They probably result from either Ca^{2+} entry through voltage-gated Ca^{2+} channels during activity mediated by Ca^{2+}-dependent or TTX-insensitive Na^+-

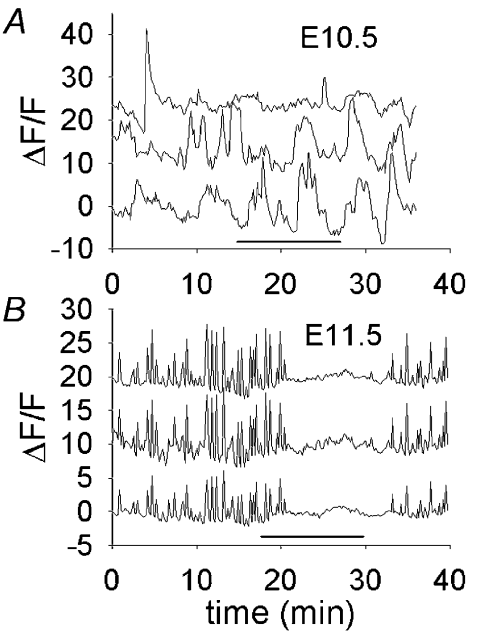

Figure 6. Later stage $[Ca^{2+}]_i$ transients are mediated by TTX-sensitive Na^+ channel-dependent events, while earlier stage transients are not

A, traces are offset vertically for better visibility. E10.5 embryo before, during and after application of 300 nM TTX (during horizontal black bar). $[Ca^{2+}]_i$ transients are not substantially affected by TTX. *B*, E11.5 embryo before, during and after application of 150 nM TTX (during horizontal black bar) which reversibly blocks all $[Ca^{2+}]_i$ transients.

dependent activity, or Ca^{2+} release from internal stores. The later-developing short-duration $[Ca^{2+}]_i$ events are probably generated by the activation of newly expressed TTX-sensitive Na^+ channels, as the sensitivity of $[Ca^{2+}]_i$ transients to TTX changes from E10.5 to E11.5. The properties and classes of ion channel expression in many neurons change over development, often from a long-duration, Ca^{2+}-dependent action potential to a faster Na^+-dependent event. The shortening of the duration of the action potential is usually due to upregulation of K^+ currents causing repolarization (for review see Spitzer, 2002).

This same mechanism might apply in hindbrain if individual transients correspond to single action potentials. It seems more possible, however, that single $[Ca^{2+}]_i$ transients correspond to bursts of action potentials, as is the case for similar activity in the hippocampus and spinal cord (Garaschuk *et al.* 1998; O' Donovan, 1999; Saint-Amant & Drapeau, 2001). If this is the case, then the developmental decrease in the duration of the $[Ca^{2+}]_i$ transients is caused by earlier termination of bursts, which may be caused by increased expression of a current such as Ca^{2+}-stimulated K^+ current ($I_{K(Ca)}$). Bursts of action potentials terminated by $I_{K(Ca)}$ occur in embryonic zebrafish spinal neurons (Saint-Amant & Drapeau, 2001). Increased expression of $I_{K(Ca)}$ can be triggered when motor neurons form synapses on target tissues (ciliary ganglion; Dryer, 1998). Indeed, in mouse hindbrain, the growing motor neuron axons of the mandibular branch of the trigeminal nerve initially contact the trigeminal sensory ganglion at E9.5 as they exit the hindbrain and coalesce with the sensory axons. Between E9.5 and E10.5, they make contact with the myogenic cells of their target, which surround them throughout the pathfinding process (Zhang *et al.* 2000). Perhaps the contact with the myogenic tissue, although it is relatively undifferentiated, causes upregulation of $I_{K(Ca)}$.

The decrease in transient duration between E9.5–E10.0 is correlated with a decrease in the interval between transients. A relationship between these two parameters would not be surprising if the interval between transients were set by a process triggered by the burst itself. For example, changes in the intervals between $[Ca^{2+}]_i$ transients could be accomplished by cumulative inactivation of Ca^{2+} channels. In ascidian muscle, the cumulative inactivation of the immature form of high-threshold Ca^{2+} channels during burst activity defines the intervals between periods of depolarization (Dallman *et al.* 2000). In mouse hindbrain motor neurons, the earlier longer transients would allow more Ca^{2+} to enter the cell, causing both more depolarization and inactivation of Ca^{2+} channels as well as a greater activation of Ca^{2+}-dependent K^+ current, causing longer intervals between transients. With shorter transients, less activation of Ca^{2+}-dependent K^+ currents and less inactivation of Ca^{2+} channels will occur, leading to shorter intervals between transients. Thus, developmental regulation of ion channels would have major and direct effects on the rate and timing of spontaneous activity.

Possible mechanisms of synchronization

Many areas of the central nervous system, such as the neonatal neocortex (Garaschuk *et al.* 2000) and hippocampus (Garaschuk *et al.* 1998), fetal retina (Meister *et al.* 1991) and neonatal spinal cord (Saint-Amant & Drapeau, 2001; Wenner & O' Donovan, 2001), generate spontaneous activity coordinated between cells or groups of cells (for reviews, see Kandler & Katz, 1995; Ben-Ari, 2001). This activity is often present during periods of synaptic formation and may coincide with the period of time during which GABA is present as a depolarizing input (Owens *et al.* 1996).

It is not yet clear whether common mechanisms underlie the synchronization of this kind of activity in different structures of the CNS. For example, excitatory GABAergic transmission is necessary for synchronized activity in the hippocampus (Garaschuk *et al.* 1998) but not in the cortex (Garaschuk *et al.* 2000). Gap junctional communication within a pacemaker population appears to drive hippocampal spontaneous activity (Strata *et al.* 1997), and gap junctions are also required throughout the active populations of neurons in cortical activity that is triggered by TEA (Peinado, 2001). However, the role of gap junctions in cortical or retinal activity remains unclear (Roerig & Feller, 2000). Similarly, application of gap junctional blockers removes synchronized activity stimulated by higher-order neurons in mouse spinal cord, but not local coordinated activity (Hanson & Landmesser, 2003).

The fact that we can record the transition from asynchronous to synchronous activity may allow us to study the mechanisms of synchronization in hindbrain branchiomeric motor neurons in ways that are not possible in other preparations. We know, for example, that synchronization appears rather abruptly at approximately the same time as TTX sensitivity of the $[Ca^{2+}]_i$ transients. This suggests that the two may be directly related, or at least driven by a common developmental event. A direct relation might occur, for example, if the more rapidly rising and shorter duration action potentials associated with the appearance of TTX-sensitive Na^+ channels propagated more rapidly or more efficiently across gap junctions within the hindbrain circuitry.

Relation of somatic $[Ca^{2+}]_i$ transients to cranial nerve activity

The early spontaneous $[Ca^{2+}]_i$ transients or later synchronized $[Ca^{2+}]_i$ events are recorded from the somata of the motor neurons, and are probably generated by action potentials that are conducted from the somata

down the axons to the periphery. In mouse cranial nerve root recordings, Abadie *et al.* (2000) could record no activity at E9.5, but found that at E10.5, the recorded electrical activity had burst durations shorter than the $[Ca^{2+}]_i$ transients at E10.5 in the present work (1.2–6.3 s for the compound action potential compared with an average of 30 s for $[Ca^{2+}]_i$ transients), which may be partially accounted for by the time needed to remove the elevated $[Ca^{2+}]_i$ from the cytoplasm. The interburst intervals recorded from the nerve roots are similar to the interval between $[Ca^{2+}]_i$ transients recorded in the motor neuron somata (40 *vs.* 75 s). At later points when activity was coordinated between different cranial nerves or sides of the embryo (E12.5), the interburst interval was similar to that seen in the current experiments at E11.5 (110 *vs.* 90 s). Thus, although the timing is not exact, it is probable that the $[Ca^{2+}]_i$ transients reported here are reflections of somatically initiated action potentials conducted to the periphery and that the synchronization is a mechanism for coordination between groups of neurons involved in neuron–target interactions. In zebrafish, spontaneous synchronized activity is observed at 20–24 h (Saint-Amant & Drapeau, 2001). This activity occurs at a later time point than spontaneous nerve-induced lateral body movements (17 h), and after responses to sensory input are observed (21 h; Drapeau *et al.* 2002). In mouse, the synchronous activity reported here is present before the earliest spontaneous movement, seen at E12.5 (Suzue, 1996). This suggests that synchronized spontaneous activity is functionally important in the generation of circuits, in contrast to motor behaviour, since at E11.5 there is no contractile response to nerve activity.

As motor neuron axons extend and reach both their peripheral targets and their local collateral targets, the synchronized activity may stimulate the post-synaptic cells to respond, inducing synapse formation. Although this is a mechanism for initial synapse formation, it is not a mechanism for pruning of inappropriate synapses. In mouse spinal cord, synchronized activity correlated with gap junction expression between motor neurons is present at early postnatal times during the period of multiple innervation of the target muscles (Chang *et al.* 1999). Later, with the disappearance of gap junctions, competition between motor neurons for space on muscle influences the ability of individual synapses to survive and the adult pattern of singly innervated muscles is generated (Personius & Balice-Gordon, 2001). Electrical coupling may have an early role in mediating synchronized activity and consequent synapse formation; this coupling may be downregulated later in development to allow synapse elimination.

Role of $[Ca^{2+}]_i$ transients in development

Spontaneous activity during development is involved in neuronal migration (Komuro & Rakic, 1998), regulation of transmitter phenotype and differentiation (Gu & Spitzer, 1994) and axonal elongation and pathfinding (Catalano & Shatz, 1998). Spontaneous activity has the direct consequence of generating $[Ca^{2+}]_i$ transients in developing neurons and different frequencies and shapes of $[Ca^{2+}]_i$ transients modulate discrete developmental events. In amphibian spinal neurons, longer duration, frequent axonal $[Ca^{2+}]_i$ waves are involved in regulation of growth cones and pathfinding, while shorter duration infrequent $[Ca^{2+}]_i$ spikes alter gene expression (Spitzer, 2002). In T lymphocytes, the frequency of $[Ca^{2+}]_i$ oscillations determines which subset of genes will be transcribed (Dolmetsch *et al.* 1998), while in B lymphocytes, the amplitude and duration of $[Ca^{2+}]_i$ signals differentially regulates transcription factors (Dolmetsch *et al.* 1997). Ca^{2+} entry through voltage-gated L-type Ca^{2+} channels preferentially drives brain-derived neurotrophic factor (BDNF) expression in cultured rat embryonic neurons; in contrast, $[Ca^{2+}]_i$ transients similar in size and duration are caused by NMDA-receptor or N-type Ca^{2+} channel activation, but do not alter Brain Derived Neurotrophic Factor gene expression (Ghosh *et al.* 1994; West *et al.* 2001). Molecular events in the periphery may have an important role in stimulating the onset of electrical activity in these cranial motor neurons and signal the progress of developmental events such as synapse formation. Chick branchiomeric motor neuron axons express EphA3 and EphA4 receptor tyrosine kinases at time points when axons are projecting peripherally to their targets and ligands for these receptors are expressed in the pathway the axons will take (Kury *et al.* 2000). Stimulation of Eph receptors by ligand has been shown to upregulate Ca^{2+} flux through NMDA receptor channels, increasing signals directing transcriptional events (West *et al.* 2001; Takasu *et al.* 2002). Thus the changes we observe, from long duration infrequent $[Ca^{2+}]_i$ events to shorter duration events may reflect different developmental roles of the $[Ca^{2+}]_i$ transients at these different stages and may assimilate input from peripheral cells or targets that further influence the developmental roles that $[Ca^{2+}]_i$ transients may play in building connected circuits.

REFERENCES

Abadie V, Champagnat J & Fortin G (2000). Branchiomotor activities in mouse embryo. *NeuroReport* **11**, 141–145.

Ben-Ari Y (2001). Developing networks play a similar melody. *Trends in Neurosci* **24**, 353–360.

Catalano SM & Shatz CJ (1998). Activity-dependent cortical target selection by thalamic neurons. *Science* **281**, 559–562.

Chang Q, Gonzalez M, Pinter MJ & Balice-Gordon RJ (1999). Gap junctional coupling and patterns of connexin expression among neonatal rat lumbar spinal motor neurons. *J Neurosci* **19**, 10813–10826.

Dallman JE, Dorman JB & Moody WJ (2000). Action potential waveform voltage clamp shows significance of different Ca^{2+} channel types in developing ascidian muscle. *J Physiol* **524**, 375–386.

Dolmetsch RE, Lewis RS, Goodnow CC & Healy JI (1997). Differential activation of transcription factors induced by Ca^{2+} response amplitude and duration. *Nature* **386**, 855–858.

Dolmetsch RE, Xu K & Lewis RS (1998). Calcium oscillations increase the efficiency and specificity of gene expression. *Nature* **392**, 933–936.

Drapeau P, Saint-Amant L, Buss RR, Chong M, McDearmid JR & Brustein E (2002). Development of the locomotor network in zebrafish. *Prog Neurobiol* **68**, 85–111.

Dryer SE (1998). Role of cell-cell interactions in the developmental regulation of Ca^{2+}-dependent K^+ currents in vertebrate neurons. *J Neurobiol* **37**, 23–36.

Easter SS Jr, Ross LS & Frankfurter A (1993). Initial tract formation in the mouse brain. *J Neurosci* **13**, 285–299.

Ericson J, Thor S, Edlund T, Jessell TM & Yamada T (1992). Early stages of motor neuron differentiation revealed by expression of homeobox gene Islet-1. *Science* **256**, 1555–1560.

Fortin G, Champagnat J & Lumsden A (1994). Onset and maturation of branchio-motor activities in the chick hindbrain. *NeuroReport* **5**, 1149–1152.

Fortin G, Kato F, Lumdsen A & Champagnat J (1995). Rhythm generation in the segmented hindbrain of chick embryos. *J Physiol* **486**, 735–744.

Fraser S, Keynes R & Lumdsen A (1990). Segmentation in the chick embryo hindbrain is defined by cell lineage restrictions. *Nature* **344**, 431–435.

Garaschuk O, Hanse E & Konnerth A (1998). Developmental profile and synaptic origin of early network oscillations in the CA1 region of rat neonatal hippocampus. *J Physiol* **507**, 219–236.

Garaschuk O, Linn J, Eilers J & Konnerth A (2000). Large-scale oscillatory calcium waves in the immature cortex. *Nat Neurosci* **3**, 452–4459.

Ghosh A, Carnahan J & Greenberg ME (1994). Requirement for BDNF in activity-dependent survival of cortical neurons. *Science* **263**, 1618–1623.

Glover JC (2000). Development of specific connectivity between premotor neurons and motoneurons in the brain stem and spinal cord. *Phys Rev* **80**, 615–647.

Gu X & Spitzer NC (1994). Spontaneous neurons calcium spikes and waves during early differentiation. *J Neurosci* **14**, 6325–6335.

Guthrie S (1996). Patterning the hindbrain. *Curr Opin Neurobiol* **6**, 41–48.

Guthrie S & Lumsden A (1992). Motor neuron pathfinding following rhombomere reversals in the chick embryo hindbrain. *Development* **114**, 663–673.

Hanson MG & Landmesser LT (2003). Characterization of the circuits that generate spontaneous episodes of activity in the early embryonic mouse spinal cord. *J Neurosci* **23**, 587–600.

Jacquin TD, Sadoc G, Borday V & Champagnat J (1999). Pontine and medullary control of the respiratory activity in the trigeminal and facial nerves of the newborn mouse: an *in vitro* study. *Eur J Neurosci* **11**, 213–222.

Jiang X, Johnson RR & Burkhalter A (1993). Visualization of dendritic morphology of cortical projection neurons by retrograde axonal tracing. *J Neurosci Meth* **50**, 45–60.

Jungbluth S, Willecke K & Champagnat J (2002). Segment-specific expression of connexin31 in the embryonic hindbrain is regulated by Krox20. *Dev Dyn* **223**, 544–551.

Kandler K & Katz LC (1995). Neuronal coupling and uncoupling in the developing nervous system. *Curr Opin Neurobiol* **5**, 98–105.

Komuro H & Rakic P (1998). Orchestration of neuronal migration by activity of ion channels, neurotransmitter receptors, and intracellar Ca^{2+} fluctuations. *J Neurobiol* **37**, 110–130.

Kury P, Gale N, Connor R, Pasquale E & Guthrie S (2000). Eph receptors and ephrin in cranial motor neurons and the branchial arches of the chick embryo. *Mol Cell Neurosci* **15**, 123–140.

Lumsden A (1990). The cellular basis of segmentation in the developing hindbrain. *Trends Neurosci* **13**, 329–335.

Lumsden A & Keynes R (1989). Segmental patterns of neuronal development in the chick hindbrain. *Nature* **337**, 424–428.

Mastick GS & Easter SS Jr (1996). Initial organization of neurons and tracts in the embryonic mouse fore- and midbrain. *Dev Biol* **173**, 79–94.

Meister M, Wong RO, Baylor DA & Shatz CJ (1991). Synchronous bursts of action potentials in ganglion cells of the developing mammalian retina. *Science* **252**, 939–943.

Moody SA, Quigg MS & Frankfurter A (1987). Development of the peripheral trigeminal system in the chick revealed by an isotype-specific anti-beta-tubulin monoclonal antibody. *J Comp Neurol* **279**, 567–580.

O' Donovan MJ (1999). The origin of spontaneous activity in developing networks of the vertebrate nervous system. *Curr Opin Neurobiol* **9**, 94–104.

Owens DF, Boyce LH, Davis MB & Kriegstein AR (1996). Excitatory GABA responses in embryonic and neonatal cortical slices demonstrated by gramicidin perforated-patch recordings and calcium imaging. *J Neurosci* **16**, 6414–6423.

Peinado A (2001). Immature neocortical neurons exist as extensive syncitial networks linked by dendrodendritic electrical connections. *J Neurophysiol* **85**, 620–629.

Personius KE & Balice-Gordon RJ (2001). Loss of correlated motor neuron activity during synaptic competition at developing neuromuscular synapses. *Neuron* **31**, 395–408.

Pierce ET (1973). Time of origin of neurons in the brain stem of the mouse. *Prog Brain Res* **40**, 53–65.

Reiner A, Veenman CL, Medina L, Jiao Y, Del Mar N & Honig MG (2000). Pathway tracing using biotinylated dextran amines. *J Neurosci Meth* **103**, 23–37.

Roerig B & Feller MB (2000). Neurotransmitters and gap junctions in developing neural circiuts. *Brain Res Rev* **32**, 86–114.

Saint-Amant L & Drapeau P (2001). Synchronization of an embryonic network of identified spinal interneurons solely by electrical coupling. *Neuron* **31**, 1035–1046.

Spitzer NC (2002). Activity-dependent neuroal differentiation prior to synaptic formation: the functions of calcium transients. *J Physiol* (*Paris*) **96**, 73–80.

Strata E, Atxori M, Molnar M, Ugolini G, Tempia F & Cherubini E (1997). A pacemaker current in dye-coupled hilar interneurons contributes to the generation of giant depolarizing GABAergic potentials in developing hippocampus. *J Neurosci* **17**, 1435–1446.

Suzue T (1996). Movement of mouse fetuses in early stages of neural development studied *in vitro*. *Neurosci Lett* **218**, 131–134.

Takasu MA, Dalva MB, Zigmond RE & Greenberg ME (2002). Modulation of NMDA receptor-dependent calcium influx and gene expression through EphB receptors. *Science* **295**, 491–495.

Trainor PA & Krumlauf R (2001). Hox genes, neural crest cells and branchial arch patterning. *Curr Opin Cell Biol* **13**, 698–705.

Valera-Echavarria A, Pfaff SL & Guthrie S (1996). Differential expression of LIM homeobox genes among motor neuron subpopulations in the developing chick brain stem. *Mol Cell Neurosci* **8**, 242–257.

Wenner P & O' Donovan MJ (2001). Mechanisms that initiate spontaneous network activity in the developing chick spinal cord. *J Neurophysiol* **86**, 1481–1498.

West AE, Chen WG, Dalva MB, Dolmetsch RE, Kornhauser JM, Shaywitz AJ, Takasu MA, Tao X & Greenberg ME (2001). Calcium regulation of neuronal gene expression. *Proc Natl Acad Sci U S A* **98**, 11024–11031.

Zhang L, Yoshimura Y, Hatta T & Otani H (2000). Reconstructing the pathway of the tensor veli palatini motor nerve during early mouse development. *Anat Embryol* **201**, 235–244.

Acknowledgements

This work was supported in part by National Science Foundation ADVANCE Cooperative Agreement SBE-0123552. It was also supported by an Howard Hughes Undergraduate Research Internship to J. G. and Mary Gates Research Training Grants to J. J. W. and E.B. P. The authors would like to thank Drs Bertil Hille, William Moody and Ed Rubel for commenting on the manuscript, and Dr Tom Daniel for considerable help with the Matlab programming. Dedicated to the memory of James F. Bosma (1916–2001).